Journal of Manufacturing Engineering, September 2016, Vol. 11, Issue. 3, pp 126-134

MODELING OF CUTTING FORCES FOR FINISHING AND ROUGHING OPERATIONS IN OBLIQUE CUTTING

***Rathod K B[1] and Lalwani D I[2]**

[1]Research scholar, [2] Associate Professor
Mechanical Engineering Department, Sardar Vallabhbhai National Institute of Technology, Surat, India.

ABSTRACT

This paper deals with the development of a predictive cutting force model for oblique cutting (3D) through the extension of an orthogonal (2D) force model of Oxley's predictive machining theory. The force model for oblique cutting is developed for finishing and roughing operations using a method described by Arsecularatne et al. (1995; 1998) that requires the orthogonal cutting forces, i.e., cutting force (FC) and thrust or feed force (FT) values, cutting edge geometry and cutting conditions (cutting speed, feed rate and depth of cut). The cutting forces are predicted from Oxley's predictive machining theory for forces, stresses, and temperatures at shear and tool-chip interface zone using Johnson and Cook flow stress model. The developed force model for oblique cutting is verified by the available literature data for AISI 4142 steel and two hot work steels, namely, AISI H 13 and AISI H 11. The predicted cutting force model shows reasonably good agreement with experiment results for oblique cutting.

Keywords: *chip flow angle, oblique tool geometries, Johnson and Cook material constants, cutting Forces.*

1. Introduction

The forces induced during machining process is not only important to understand the process of chip formation but also useful in design of cutting tools, selection of cutting conditions, design of jigs and fixtures and design of machine tool structures. Therefore, cutting forces are required to study and wide research has been carried out in the past by many researchers. One of the most widely used analytical models for orthogonal cutting is Oxley's predictive machining theory that is based on the chip formation model and derived from the slip line field analysis and the strain rate analysis of experimental flow fields. The Oxley's predictive machining theory of chip formation is extended by the many researchers (Adibi-Sedeh et al., 2003; Karpet and Ozel, 2006; Lalwani et al., 2009; Chen et al., 2015) to predict the forces, stresses and temperatures at shear plane and at tool-chip interface using Johnson and Cook material model during orthogonal cutting.

There are numbers of practical machining processes of chip formation in which cutting edge is not set normal to the cutting velocity but inclined at an angle (known as inclination angle), then the machining process is called oblique cutting. The oblique cutting differs from orthogonal cutting process mainly indirection of chip flow over the tool face making an to predict the cutting force components in oblique cutting, it is first necessary to have the knowledge of chip flow angle. Several attempts have been made to predict chip flow angle with nose radius tool by Colwell (1954), Okushima and Minato (1959), Lin et al., (1982); they assumed both inclination and rake angle of the tool is zero (0°). Van Luttervelt and Pekelharing (1976) and Kluft et al. (1979) analysed the effect of cutting conditions (feed rate and depth of cut) on the chip flow angle and showed that the chip flow angle in oblique cutting depends upon the tool geometry, cutting conditions and workpiece curvature. Young et al. (1987) developed the mathematical model to predict chip flow angle by considering the effect of the nose radius of a tool. They developed the chip flow model and treated the chip as a series of independent element of infinitesimal width (Fig. 1). The thickness and orientation of chip section corresponding to each chip element varies, therefore the friction force component of element at the cutting edge also varies in magnitude and direction. The friction force of all elements are then summed up to find their resultant and assumed that the direction of the resultant friction force is the direction of chip flow. Then, chip flow angle due to nose radius tool is determined based on geometric consideration (Fig. 1).

**Corresponding Author - E- mail: kbr.fetr@gmail.com*

The same approach was extended by the Arsecularatne et al. (1995) for roughing machining and Arsecularatne et al. (1998) for finish machining in oblique cutting to calculate the chip flow angle and cutting forces.

In the present work, the aim is to develop cutting force model, which can predict forces induced during roughing and/or finish operations in oblique cutting (3D) using the method described by Arsecularatne et al. (1995; 1998). The developed cutting force model was tested for three different materials for which the data are available in literature, namely, AISI 4142 steel, AISI H13 and AISI H11 steel. The brief description and procedure of force modeling in oblique cutting is given in next section.

2. Force modeling in oblique cutting

The oblique force modeling is an extension of orthogonal force model. In predicting the orthogonal force components, Oxley's predictive machining theory of chip formation is used. The Johnson and Cook (JC) flow stress model is used to represent the workpiece material properties instead of Oxley's power law material model. In the present work, a predictive cutting force model for orthogonal cutting (2D) was first build using computer program based on the iteration (loop) provided in flow chart by Lalwani et al., (2009).To estimate the orthogonal cutting forces (F_C and F_T) from 2D model requires cutting conditions, flow stress data of work material (Table 1) and thermal and physical properties of workpiece material (Table 2).

Table1. Johnson and Cook flow stress constants

Workpiece material	A (MPa)	B (MPa)	C	N	M	Tm (°C)
AISI 4142 steel [1]	598.0	768.0	0.0137	0.2092	0.807	1520
AISI H 13 steel[2]	674.8	239.2	0.027	0.28	1.3	1760
AISI H 11 steel[3]	_	835.0	0.0185	0.33	2.75	1427

[1]Al-Zkeri et al., 2009, [2]Huang and Liang, 2003, [3]Cherif M et al., 2004

Table 2. Thermal and physical properties of workpiece material

Workpiece material	Specific heat, C_p (J / kg /°C)	Thermal Conductivity, K (W/m °C)	Density, ρ(kg/m³)
AISI 4142 steel[1]	420 + 0.504T	43.18 - 0.0173T	7800
AISI H 13 steel[2]	420 + 0.504T	52.61 - 0.0281T	7760
AISI H11 steel[3]	450.8 + 0.454 T	29.46 + 0.017 T	7847

2.1 Calculation procedure for force model in oblique cutting

Arsecularatne et al. (1995; 1998) made significant contribution to predict the oblique cutting forces and chip flow angle for nose radius tool. The chip flow angle in oblique cutting is calculated based on geometric considerations and is assumed to coincide with the direction of resultant force. The chip flow angle is modelled considering the chip as a series of elements with infinitesimal width, where the thickness (t) and orientation of the uncut chip section (dA) corresponding to each chip element varies (Fig. 1a). The elemental frictional forces (dF) of each element are integrated along the cutting edge to find the resultant frictional force (F) and its direction as shown in Fig. 1(b). Thus, the chip flow angle equation (1) is obtained by integrating the numerator and denominator over the whole area of undeformed chip section and given as

$$\bar{\Omega}_o = tan^{-1}\left(\frac{\int sin\ \Omega_o dA}{\int cos\ \Omega_o dA}\right) \quad (1)$$

A schematic of a nose radius tool, when the depth of cutis such as to use only part of nose radius is shown in Fig.1(a) and when the depth of cut extends beyond the tool nose radius to include at least part of the side cutting edge is shown in Fig.1(b).

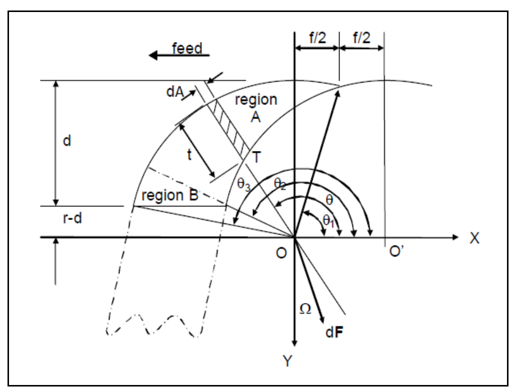

dA = area of undeformed chip element
$\theta_1,\theta_2,\theta_3$= limit of integration (degree)
= chip flow angle
dF = friction force acting on chip element
f = feed (mm/rev)
d = depth of cut (mm)
r = tool nose radius (mm)

(a) A typical nose radius tool when the depth of cut is such to use round nose part of cutting edge

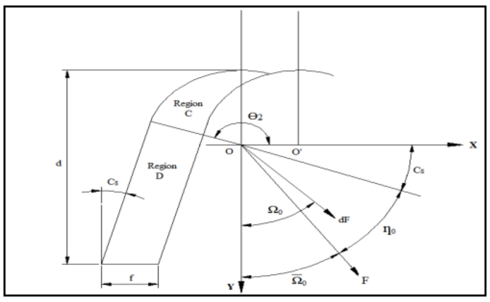

C_s = side cutting edge angle (degree)

θ_2= limit of integration (degree)

= chip flow angle (degree)

= chip flow angle due to nose radius effect measured from positive Y-axis (degree)

dF = friction force acting on chip element (N)

F = frictional force at tool-chip interface (N)

d = depth of cut (mm)

= chip flow angle due to nose radius effect measured from normal to C_s (degree)

(b)A typical nose radius tool when the depth of cut extends beyond the round nose part of cutting edge

Fig.1Geometry of chip flow model for nose radius tool (Young et al., 1987)

To obtain the results for the numerator (NUM) and denominator (DEN) of the equation (1) for both the cases as shown in Figs.1 (a) and (b), Young et al. (1987) provided following equations:

Case 1: $d \le r$ (1 −(Fig. 1a)

$$NUM = [-r\sin\theta]_{\theta_1}^{\theta_2} + \frac{1}{2}\left[\sin\theta\,(r^2 - f^2\sin^2\theta)^{1/2} + \frac{r^2}{f}\sin^{-1}\left(\frac{f}{r}\sin\theta\right)\right]_{\theta_1}^{\theta_2} + f\left[\frac{\sin 2\theta}{4} + \frac{\theta}{2}\right]_{\theta_1}^{\theta_2} + [(r-d)\log(\sin\theta)]_{\theta_2}^{\theta_3} \quad (2)$$

$$DEN = [-r\cos\theta]_{\theta_1}^{\theta_2} + \frac{1}{2}\left[\cos\theta\,(r^2 - f^2\sin^2\theta)^{1/2} + \frac{r^2-f^2}{f}\times\log\left\{(f\cos\theta) + (r^2 - f^2\sin^2\theta)^{1/2}\right\}\right]_{\theta_1}^{\theta_2} + \frac{f}{4}[\cos 2\theta]_{\theta_1}^{\theta_2} + [-(r-d)\theta]_{\theta_2}^{\theta_3} \quad (3)$$

Where the limits of integration are

$$\theta_1 = \cos^{-1}\left(\frac{f}{2r}\right)$$
$$\theta_2 = \pi - \tan^{-1}\left\{\frac{r-d}{(2rd-d^2)^{1/2} - f}\right\}$$
$$\theta_3 = \pi - \sin^{-1}\left(\frac{r-d}{r}\right) \quad (4)$$

Case 2: $d > r$ (1 (Fig. 1b)

$$NUM = [-r^2\sin\theta]_{\theta_1}^{\theta_2} + \frac{r}{2}\left[\sin\theta\,(r^2 - f^2\sin^2\theta)^{1/2} + \frac{r^2}{f}\sin^{-1}\left(\frac{f}{r}\sin\theta\right)\right]_{\theta_1}^{\theta_2} + rf\left[\frac{\sin 2\theta}{4} + \frac{\theta}{2}\right]_{\theta_1}^{\theta_2} + \left[f\{d - r(1-\sin C_s)\} - \frac{f^2}{4}\sin(2C_s)\right]\cos C_s \quad (5)$$

$$DEN = [-r^2\cos\theta]_{\theta_1}^{\theta_2} + \frac{r}{2}\left[\cos\theta\,(r^2 - f^2\sin^2\theta)^{1/2} + \frac{r^2-f^2}{f}\times\log\left\{(f\cos\theta) + (r^2 - f^2\sin^2\theta)^{1/2}\right\}\right]_{\theta_1}^{\theta_2} + \frac{rf}{4}[\cos 2\theta]_{\theta_1}^{\theta_2} + \left[f\{d - r(1-\sin C_s)\} - \frac{f^2}{4}\sin(2C_s)\right]\sin C_s \quad (6)$$

Where the limits of integration are

$$\theta_1 = \cos^{-1}\left(\frac{f}{2r}\right)$$
$$\theta_2 = \pi - C_s \quad (7)$$

Where, d is the depth of cut, f is the feed rate, r is the tool nose radius and Cs is the side cutting edge angle. For any depth of cut, the direction of chip flow because of nose radius effect can be written as

$$\bar{\Omega}_o = \tan^{-1}\left(\frac{NUM}{DEN}\right) \quad (8)$$

Where, NUM and DEN are obtained by equations (2) to (5). The chip flow angle can also be represented from a line which is normal to straight part of the side cutting edge of the tool as shown in Fig. 1 (b), if this angle is designated by and then it can be linked to as

$$\eta_o = \frac{\pi}{2} - C_s - \bar{\Omega}_o \quad (9)$$

Wang and Mathew (1988) defined the geometry of a nose radius tool through non-zero inclination angle and rake angle using a system of fundamental planes based on IS recommendations. The typical nose radius tool with its general and modified equivalent angles is shown in Fig. 2. For the proposed equivalent cutting edge of nose radius tool, three-dimensional geometric analysis technique can be used to determined equations for the fundamental planes and cutting face plane of a given tool from its basic tool angles. The equation for is obtained using three dimensional geometric analyses, which is the projection of on the tool rake face plane as shown in Fig. 2 and is obtained as

$$\eta_o' = \; = \cos^{-1}\left[\frac{\sec i - \tan i \tan\eta_o \tan\alpha_n}{\{(\tan i - \tan\eta_o \tan\alpha_n \sec i)^2 + \sec^2\eta_o\}^{\frac{1}{2}}}\right] \quad (10)$$

The other equivalent angles, such as

cutting edge rake angle (α_n^*), inclination angle (i^*) and side cutting edge angle (C_s^*), are then obtained by Wang and Mathew (1988) using geometrical relation which are given as

$$i^* = sin^{-1}(\cos\eta'_o \ \sin i - \sin\eta'_o \sin\alpha_n \cos i)$$

$$\alpha_n^* = sin^{-1}\left(\frac{\cos\eta'_o \sin i - \sin i^*}{\tan\eta'_o \ \cos i^*}\right)$$

$$C_s^* = C_s + \eta_o$$

(11)

Stabler (1951) found from the experimental results that the chip flow angle ($\overset{*}{\eta_c}$) would be equal to inclination angle in the rake face plane, which is now generally known Stabler's flow rule is given by

$$\overset{*}{\eta_c} = i^* \qquad (12)$$

The chip flow angle (η_c) is measure in the rake face plane as the angle between the normal to the straight part of the side cutting edge and direction of the chip flow, which is given as

$$\eta_c = \eta'_o + i^* \qquad (13)$$

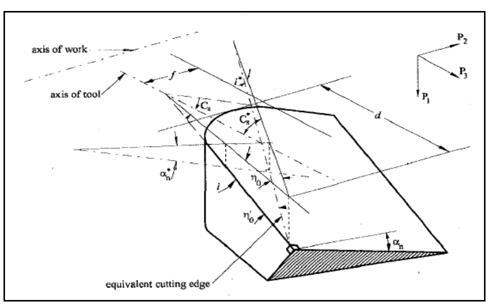

C_s = side cutting edge angle (degree)
I = inclination angle (degree)
Cs = normal rake angle (degree)
η_o= chip flow angle due to effect of the nose radius measured from the normal to side cutting edge angle and reference plane (degree)
Asterisk (*) =symbolises angles associated with equivalent cutting edge

Fig. 2 The nose radius tool with equivalent cutting edge angles (Arsecularatne et al., 1998)

Arsecularatne et al. (1998) reported that the tool manufacturer provides smallest possible edge radius based on feed range value for which the insert is used to prevent the cutting edge from chipping and also argued that this edge radius affects the nominal rake angle considerably when small feed and low depth of cut are used. Finish hard turning is one of the metal cutting operations, where small feed and low depth of cut is generally used. Therefore, the effect of edge radius on nominal rake angle during finish turning is considerable. The method involves to find the engagement of effective cutting face of an insert is modification of the nominal rake angle considering the cutting edge radius (r_n) and undeformed chip thickness (t_1) by Arsecularatne et al. (1998). The nominal rake angle can be modified using the relation as

$$\alpha_n' = tan^{-1}\left(\frac{r_n \sin\beta - r_n \sec\alpha_n^* + (t_1 - r_n)\,\mathrm{ta}}{t_1 - r_n(1-\cos\beta)}\right) \qquad (14)$$

Where, $\beta = \frac{\pi}{4} + \frac{\alpha_n^*}{2}$ = cutting edge radius and

α'_n = modified nominal rake angle

Arsecularatne et al. (1998) proposed an approach to predict the cutting forces for oblique machining conditions based of experimental observations. Experimental results indicated that cutting and thrust forces are very nearly independent of inclination angle. Thus, the cutting force (FC and FT) components can be determined using orthogonal conditions assuming zero inclination angles (i = 0º) with rake angle, $\alpha = \alpha_n^*$ irrespective of its actual value. Then, using FC and FT values, the third component, FR (i.e., resultant cutting force which lies normal to tool face and acting in the chip flow direction) value can be found from the given values of with as given in equation (12). Therefore, the resultant force is determined by deriving an expression in terms of predicted values of FC and FT together with the tool angle equations (9), and chip flow angle equation (12) result into non-zero inclination as

$$F_R = \frac{F_C\,(sin i^* - cos i^* sin\alpha'_n tan\eta^*_c) - F_T\, cos\alpha'_n\, tan\eta^*_c}{sin\, i^*\, sin\alpha'_n tan\eta^*_c + \ cos i^*} \qquad (15)$$

Where F_C is the force in cutting direction, F_T is force normal to cutting direction and machined surface, F_R is resultant force of F_C and F_T, i^* is the inclination angle, α_n' modified normal rake angle and η^*_c is chip flow direction. This equation is used for finish turning operation and can be used for rough machining by replacing α_n' to α_n^*.

In oblique cutting, the cutting edge and cutting velocity is rotated, so that Cs≠ 0º. Therefore, forces F_T and F_R no longer act in feed and radial directions and it is usual to redefine the forces acting on the tool as P_1, P_2 and P_3,where these forces act in the cutting, feed (axial), and radial direction respectively [12,18] as given below:

$$
\begin{aligned}
P_1 &= F_C \\
P_2 &= F_T \ \cos C_s^* + F_R \ \sin C_s^* \\
P_3 &= F_T \ \sin C_s^* - F_R \ \cos C_s^*
\end{aligned}
\tag{16}
$$

3. Results and discussion

The orthogonal and oblique cutting force models are developed using Matlab® and flow chart is shown in Fig. 3. The inputs for the model are predicted F_C and F_T values from orthogonal force model, cutting conditions, and tool geometry to estimate the cutting force components in oblique cutting. The three work materials, i.e., AISI 4142 steel, two hot work steels AISI H13 and AISI H 11, are used to predict cutting force components in oblique cutting. The results obtain are presented in next section.

3.1 AISI 4142 steel

Moufki et al. (2004) presented the experimental force results during oblique cutting of AISI 4142 (42CrMo4) steel using uncoated Tic tools. The tool holder selected for mounting insert was PTGNR2020K16 which results into tool geometry as normal rake angle (α_n) = 0°, major cutting edge angle (χ_r) = 91° and nose radius (r) = 0.4 mm. The side cutting edge angle (C_S) is calculated as 90° - major cutting edge angle (χ_r). The cutting conditions for oblique cutting tests are taken as cutting speed (V) = 60 m/min, depth of cut (d) = 3 mm at different feed rates with two different inclination angle (Moufki et al., 2004). The average edge radius value (r_n) for carbide tool is taken as 0.012 mm (Arsecularatne et al., 1998).

Table 3 shows comparison between experiment results published by Moufki et al. (2004) and predicted results by the proposed force model. It is clear from Fig.4 that as the feed rate increases, the cutting forces also increases. This can be due to the fact that as the feed rate increases, the volume of work material comes in contact with the cutting tool increases, therefore high cutting forces are required to shear the metal (Suresh et al., 2012). Fig. 4 depicts that as the feed rate increases, all the three components force increase for both inclination angles (i = 5º and 10º) but keeping the feed rate constant and varying the inclination angle, the cutting force (P_1) and feed force (P_2) decreases, whereas radial force (P_3) increases. The predicted results for three force components P_1 (cutting force), P_2 (feed force) and P_3 (radial force) seem to be reasonably good agreement with the experimentally measured forces of Moufki et al. (2004). For 5º inclination angle, the average absolute error for cutting force (P_1) = 7.61%, the feed force (P_2) = 16.92% and the thrust force (P_3) = 24.16% and for inclination angle, i = 10º, P_1 = 3.61%, P_2 = 8.81% and P_3 = 28.01%.

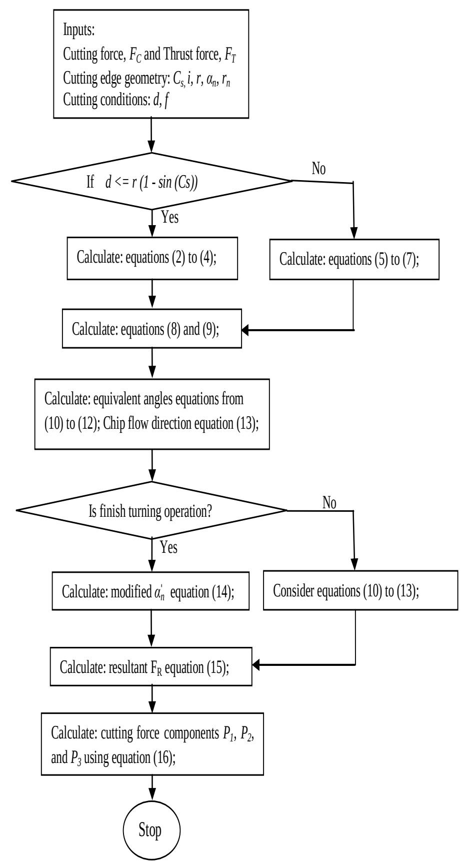

Fig. 3 Flow chart for oblique cutting based on Arsecularatne theory

Table3. Comparison of experimental results (*V* = 60 m/min, d = 3.0 mm, α = 0º) of Moufki et al. (2004) with predicted results of cutting forces for AISI 4142 steel

Test	Inclination angle (degree)	f (mm/rev)	Experimental			Predicted		
			P_1 (N)	P_2 (N)	P_3 (N)	P_1 (N)	P_2 (N)	P_3 (N)
1	i = 5º	0.1	920	714	33	824.03	554.45	22.71
2		0.15	1202	821	48	1127.3	691.9	36.66
3		0.25	1800	1042	56	1688.7	909.85	65.89
1	i = 10º	0.1	882	686	86	824.03	554.45	41.25
2		0.15	1115	715	90	1127.3	691.9	68.45
3		0.25	1637	948	137	1688.7	909.85	125.97

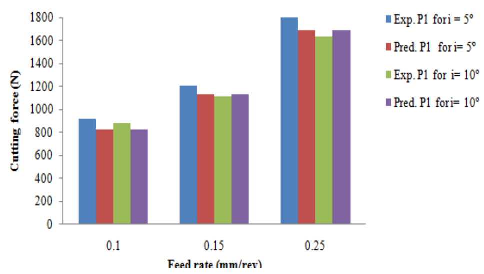

(a) Comparision of experimental results of cutting force (P_1) with proposed force model

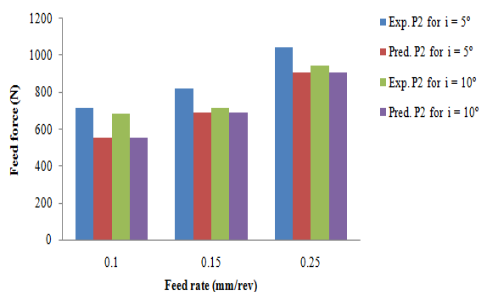

(b) Comparision of experimental results of feed force (P_2) with proposed force model

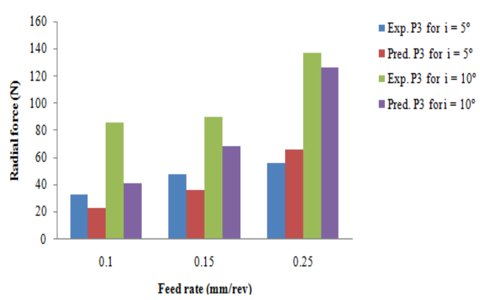

(c) Comparision of experimental results of radial force (P_3) with proposed force model

Fig. 4 Comparison of experimental results of AISI 4142 steel (Moufki et al., 2004) with predicted results of cutting force

3.2 AISI H13 steel

The hard turning experiments of AISI H13 steel using ceramic inserts were conducted by Suresh et al. (2012) to develop cutting forces model. The tool holder selected for mounting ceramic insert was PCLNL2525M12 which results in to tool geometry as rake angle (α = -6°), major cutting edge angle (χ_r = 95°), nose radius (r = 0.8) mm and inclination angle (i = -6°). The average edge radius value (r_n) for ceramic tool is taken as 0.025 mm (Coelho, 2004).

Table 4 shows experiment results of AISI H13 proposed by Suresh et al.(2012) with predicted results of the proposed cutting force. The influence of cutting speed (V) on actual and predicted values of cutting forces is shown in Fig. 5.The predicted results for three force components P_1, P_2 and P_3 seem to be reasonably good agreement with the experimentally measured forces of Suresh et al. (2012).The average absolute error found for cutting force is (P_1) = 2.51%, the feed force (P_2) = 27.60% and the radial force (P_3) = 49.22%. Fig. 5 shows that as cutting speed increases (keeping feed and depth of cut constant); the predicted values of cutting forces decreases and experimental results confirm the same. In this regard, Suresh et al. (2012) reported that decreasing trends of cutting forces with increase in cutting speed is due to increase in temperature at the shear zone, resulting in plastic softening of machined surface and also the strength of material.

Table 4. Experimental results reported by Suresh et al. (2012) (keeping *d* = 0.4 mm and *f* = 0.14 mm/rev constant) and predicted results of cutting forces for AISI H13model

Test	V (m/min)	Experimental			Predicted		
		P_1 (N)	P_2 (N)	P_3 (N)	P_1 (N)	P_2 (N)	P_3 (N)
1	80	158	94	170	161.04	74.80	100.04
2	140	148	82	158	140.91	57.61	75.75
3	200	130	74	142	131.06	49.85	64.69

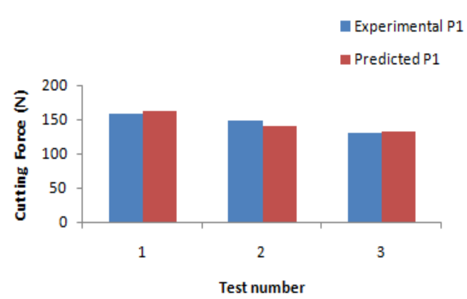

(a) Comparision of experimental results of cutting force (P_1) with proposed force model

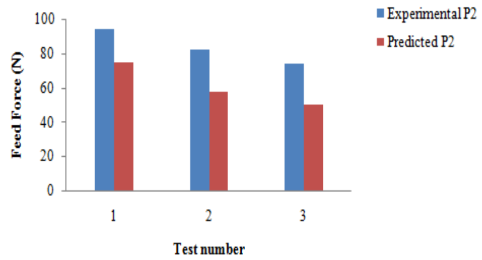

(b) Comparision of experimental results of cutting force (P_2) with proposed force model

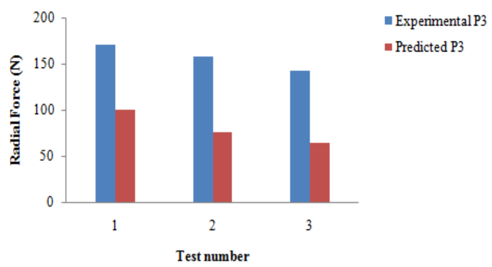

(c) Comparision of experimental results of cutting force (P_3) with proposed force model

Fig. 5 Comparison between predicted results of cutting forces with the experimental results of AISI H13 steel (Suresh et al., 2012)

3.3 AISI H11 steel

Fig. 6 shows the comparison of predicted values of cutting force components with experimentally obtained values of AISI H11 steel by Aouici et al. (2012).The finish hard turning experiments of AISI H11steel carried out with CBN tools (SNGA120408 S01020) using different feed rates and depth of cut with constant cutting velocity (*V* =180 m/min) are shown in Table 5.The tool holder selected for mounting CBN insert was PSBNR 2525 K12 which results in to tool geometry as rake angle (α = -6°), major cutting edge angle (χ_r=75°), nose radius (r = 0.8 mm) and inclination angle (i = -6°) Aouici et al., 2012.The average edge radius value (r_n) for CBN tool was taken as 0.02 mm (Thiele and Melkote, 1999).

The predicted values of cutting force components P_1, P_2 and P_3 seem to be reasonably good agreement with experimentally obtained values of cutting forces by Aouici et al. (2012). The average absolute error found for cutting force (P_1) is 2.24%, the feed force (P_2) is 17.25% and the radial force (P_3) is 28.10%.

Table 5.Experimentalresults of AISI H11 steel keeping *V* =180 m/min constant (Aouici et al., 2012) and predicted results of cutting forces

Test	f (mm/rev)	d (mm)	Experimental			Predicted		
			P_1 (N)	P_2 (N)	P_3 (N)	P_1 (N)	P_2 (N)	P_3 (N)
1	0.16	0.45	252.08	147.22	247.77	248.04	129.24	169.25
2	0.12	0.45	222.92	166.95	228.22	216.41	125.09	157.29
3	0.08	0.3	122.83	90.81	160.47	119.67	63.80	104.25
4	0.12	0.3	147.03	66.33	135.42	144.27	67.65	115.63

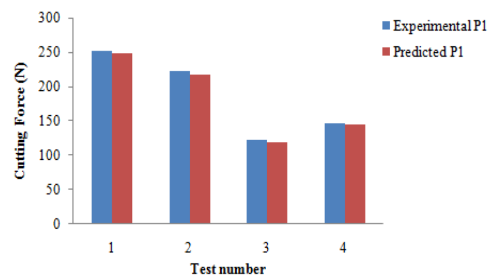

(a) Comparison of experimental results of cutting force (P_1) with proposed force model

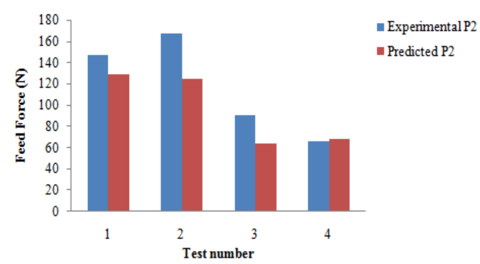

(b) Comparision of experimental results of cutting force (P_2) with proposed force model

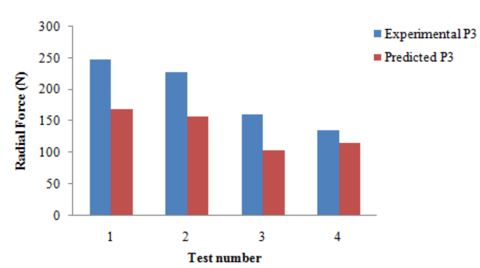

(c) Comparision of experimental results of cutting force (P_3) with proposed force model

Fig. 6 Comparison between predicted cutting forces results with the experimental results of AISI H11 steel (Aouici et al., 2012)

4. Conclusions

The present work is aimed to develop oblique cutting model for predicting cutting forces for three materials using Oxley's predicative machining theory and Arsecularatne method (1995; 1998) of chip flow direction and cutting forces. The oblique cutting force model is an extension of orthogonal cutting model. The orthogonal force model is developed by the procedure described by Lalwani (2009) that is based on Oxley's predictive machining theory and Johnson and Cook flow stress model. The accuracy of orthogonal cutting and oblique cutting model depend upon the knowledge of cutting conditions, tool geometry, work material properties, temperature dependent thermal properties and flow stress properties of work material. The developed force models are tested with the experimental data available in literature for AISI 4142 steel, AISI H13 and AISI H11 steel. The results generated by the force model are compared with published experimental results of different researchers and they are found in reasonably good agreement.

References

1. *Adibi-Sedeh A H Madhavan Vand Bahr B (2003), "Extension of Oxley's analysis of machining to use different material models", Journal of Manufacturing Science and Engineering, Vol.125, 656- 666.*

2. *Aouici H Yallese M A Chaoui K Mabrouki T and Rigal J F (2012), "Analysis of surface roughness and cutting force components in hard turning with CBN tool: Prediction model and cutting conditions optimization", Measurement, Vol. 45, 344–353.*

3. *Arsecularatne J A Fowle R F and Mathew P (1998), "Prediction of chip flow direction, cutting forces and surface roughness in finish turning", Journal of manufacturing science and engineering, Vol. 120,1-12.*

4. *Arsecularatne J A Mathew P and Oxley P L B (1995), "Prediction of chip flow direction and cutting forces in oblique machining with nose radius tools", Proceedings of the Institution of Mechanical Engineers, Vol. 209, 305-315.*

5. *Chen Y Li H and Wang J (2015), "Further development of Oxley's predictive force model for orthogonal cutting", Machining Science and Technology, An international journal, Vol.19, 86-111.*

6. *Cherif M Thomas H Furet B and Hascoet J Y (2004), "Generic modeling of milling forces for CAD/CAM applications" International Journal of Machine Tools & Manufacture, Vol. 44, 29–37.*

7. *Chinchanikar S and Choudhury S K (2016), Cutting force modeling considering tool wear effect during turning of hardened AISI 4340 alloy steel using multi-layer TiCN/Al2O3/TiN-coated carbide tools", The International journal of Advance manufacturing Technology, Vol. 83 (9), 1749 – 1762.*

8. *Coelho R T Silva L R Braghini A and Bezerra A A (2004), "Some effects of cutting edge preparation and geometric modifications when turning INCONEL 718TM at high cutting speeds", Journal of Materials Processing Technology, Vol. 148,147–153.*

9. *Colwell L V (1954), "Predicting the angle of chip flow for single point tools", Transactions ASME, Vol. 76, 199-204.*

10. *Huang Y and Liang S Y (2003), "Cutting forces modeling considering the effect of tool thermal property-application to CBN hard turning", International journal of machine Tools & Manufacture, Vol. 43,307-315.*

11. *Jaspers S P F C and Dautzenberg J H (2002), "Material behavior in conditions similar to metal cutting: flow stress in the primary shear zone", Journal of Materials Processing Technology, Vol. 122, 322–330.*

12. *Jiann-Cherng Su (2006), Ph. D thesis on Residual stress modeling in machining processes, George W Woodruff school of mechanical engineering, Georgia Institute of Technology.*

13. *Karpat Y and Ozel T (2006), "Predictive analytical and thermal modelling of Orthogonal Cutting Process, Part I Predictions of tool forces, stresses, and temperature distributions", Journal of Manufacturing Science and Engineering, Vol. 128,435–444.*

14. *Kluft W Konig W van Luttervelt C A Nakayama K and Pekelharing A J (1979), "Present knowledge of chip control", Annal CIRP, Vol.28 (2), 441-445.*

15. *Lalwani D I Mehta N K Jain P K (2009), "Extension of Oxley's predictive machining theory for Johnson and cook flow stress model", Journal of Materials Processing Technology, Vol. 209 (12-13), 5305-5312.*

16. *Okushima K and Minato K (1959), "On the behavior of chip in steel cutting", Bulletin of the Japan Society of Mechanical Engineers, Vol. 2(5), 58-64.*

17. *Oxley P L B (1989), "The mechanics of machining: An analytical approach to assessing machinability", Ellis Horwood Ltd, England.*

18. *Qayyum F Shah M Manzoor S and Abbas M (2015), "Comparison of thermo mechanical stresses produced in work rolls during hot and cold rolling of Cartridge Brass 1101", Materials Science and Technology, Vol. 31(3), 317-324.*

19. *Spaans C and van Geel P F H J (1970), "Break mechanism in cutting with a chip breaker", Annals of the CIRP, Vol. 18,87-92.*

20. *Suresh R Basavarajappa S and Samuel G L (2012), "Predictive modeling of cutting forces and tool wear in hard turning using response surface methodology", International conference on modeling optimization and computing Procedia engineering, Vol. 38,73-81.*

21. *Thiele J D and Melkote S N (1999), "Effect of cutting edge geometry and workpiece hardness on surface generation in the finish hard turning of AISI 52100 steel", Journal of Materials Processing Technology, Vol. 94,216–26.*

22. *Usui E and Hirota A (1978), "Analytical prediction of three dimensional cutting process Part II: chip formation and cutting force with conventional single point tool", Transactions ASME, Vol. 100, 229-235.*

23. *Van Luttervelt C A and Pekelharing A J (1976), "Chip formation in machining operation at small diameter", Annal CIRP, Vol. 25(1), 71-76.*

24. *Wang J and Mathew P (1988), "Predicting the chip flow direction for nose radius tools under oblique machining conditions", University of New South Wales report 1988/IE/2.*

25. *Young H T Mathew P and Oxley P L B (1987), "Allowing for nose radius effects in predicting the chip flow direction, and cutting forces in bar turning", Proceedings of the Institution of Mechanical Engineers, Part C, Vol.201,213-226.*

